

# **Endo-fullerene and Doped Diamond Nanocrystallite based Models of Qubits for Solid-State Quantum Computers**

Seongjun Park  
Department of Chemical Engineering  
Stanford University, Stanford, CA 94305-5025

Deepak Srivastava\*  
Computational Nanotechnology at CSC/NAS  
NASA Ames Research Center, Moffett Field, CA 94035-1000

Kyeongjae Cho  
Department of Mechanical Engineering  
Stanford University, Stanford, CA 94305-4040

\* Author to whom correspondence should be addressed: [deepak@nas.nasa.gov](mailto:deepak@nas.nasa.gov)

## **Abstract:**

Models of encapsulated  $\frac{1}{2}$  nuclear spin  $^1\text{H}$  and  $^{31}\text{P}$  atoms in fullerene and diamond nanocrystallite, respectively, are proposed and examined with *ab-initio* local density functional method for possible applications as single quantum bits (qubits) in solid-state quantum computers. A  $^1\text{H}$  atom encapsulated in a fully deuterated fullerene,  $\text{C}_{20}\text{D}_{20}$ , forms the first model system and *ab-initio* calculation shows that  $^1\text{H}$  atom is stable in atomic state at the center of the fullerene with a barrier of about 1 eV to escape. A  $^{31}\text{P}$  atom positioned at the center of a diamond nanocrystallite is the second model system, and  $^{31}\text{P}$  atom is found to be stable at the substitutional site relative to interstitial sites by 15 eV. Vacancy formation energy is 6 eV in diamond so that substitutional  $^{31}\text{P}$  atom will be stable against diffusion during the formation mechanisms within the nanocrystallite. The coupling between the nuclear spin and weakly bound (valance) donor electron coupling in both systems is found to be suitable for single qubit applications, where as the spatial distributions of (valance) donor electron wave functions are found to be preferentially spread along certain lattice directions facilitating two or more qubit applications. The feasibility of the fabrication pathways for both model solid-state qubit systems within practical quantum computers is discussed with in the context of our proposed solid-state qubits.

## **Introduction:**

Quantum computers promise to exceed the computational efficiency of present day classical computers because quantum algorithms allow the execution of certain tasks in much fewer numbers of steps. Ones and zeros (bits) of classical computers are replaced by quantum states of a two level system – a qubit. Logical operations are performed on qubits and their measurement determines the result. [1] Interest in quantum computations has recently increased dramatically because of two reasons. First, efficient quantum algorithms for prime factorization and exhaustive data base searches have been developed. [2,3] Second, quantum error correcting codes have been developed that allow the operation of a quantum computer with a certain degree of de-coherence in the quantum state, i.e., the quantum states need not be so coherent as they were thought previously. [4] The main difficulty is in realizing two-level quantum systems on which measurements can be made and which must be isolated from the environment as well.

Of many suggested models, the quantum states of spin  $\frac{1}{2}$  particles, such as nuclear spins, have been proposed as isolated two level quantum systems. Nuclear spin resonance approach, through nuclear magnetic resonance (NMR) experiments on bulk liquids, allows quantum computations by circumventing the single-spin detection problem. [5,6] Quantum computations involving a few (up to 7) qubits have been demonstrated so far but the main problem is that NMR on bulk liquids may not be scalable to more than a few qubits system. As an alternative, following the same philosophy of treating nuclear spins as isolated two level systems, conceptual design for solid-state quantum computer based on  $^{31}\text{P}$  donor atoms dopants in bulk silicon has been proposed by Kane. [7] The nuclear spin of a single  $^{31}\text{P}$  donor atom in bulk silicon serves as a single qubit, and Kane has developed a scheme to control the state of the qubit through a coupling of the nuclear spin with the weakly bound donor electron of the dopant atom. The overall architecture involves making well-defined precise arrays of  $^{31}\text{P}$  donor atoms in bulk silicon. The nuclear spin states of individual qubits and the interaction between the neighboring qubits are controlled by electronic gates placed over each qubit and in the spacing between neighboring qubits. Four out of five valance electrons of a  $^{31}\text{P}$  donor atom are used up in the tetrahedral covalent bonding with the silicon lattice, whereas the fifth donor electron exists

in a weakly bound state with large spatial extension in the lattice. The external electronic gate over each qubit indirectly controls the nuclear spin state by manipulating the donor electron distribution leading to a change in hyperfine interaction between the nuclear spin and the weakly bound donor electron. The electronic gates between two qubits similarly modify the overlap between the neighboring donor electron wave functions and control the interactions between the neighboring qubits.

The main requirements in realizing the Kane's architecture are the placement of  $^{31}\text{P}$  dopant atoms in precise array locations, which are hundreds of nanometer beneath silicon surface layers, and the fabrication of electronic gates to control individual qubits and the interactions between them. There are major experimental challenges in realizing this architecture. The most critical is how to position dopant atoms at precise positions beneath surface layers. Additionally, during fabrication steps dopant atoms are very likely to diffuse away from initial positions due to thermal effects, and after fabrication, intrinsic defects (e.g. vacancies and self interstitials) in silicon will induce additional transient enhanced diffusion (TED) of the dopant atoms. Kane himself noted these problems and predicted that the fabrication steps "will require significant advances in the rapidly moving field of nanotechnology." [7]

In this paper we report new model systems, which can overcome the above fabrication related difficulties. Based on *ab-initio* feasibility simulations, in this work we propose and examine a possible solution that envisions using "encapsulated"  $\frac{1}{2}$  nuclear spin donor atom dopants, in fullerenes and diamond nanocrystallites, as solid-state single qubits that could be used in realizing a nuclear spin based architecture of solid-state quantum computers. Since nanocrystallite or fullerene encapsulated dopant atoms will be of larger size than the single dopant atoms, they would be easier to position and incorporate in precise locations. Furthermore, our calculations show that the dopant atoms will be structurally much more stable against any diffusion both before and after fabrication steps. In the following, we present details of the model systems for using encapsulated nuclear spin  $\frac{1}{2}$  dopant atoms as solid-state quantum bits, and the possible fabrication pathways or steps that have been already demonstrated in experiments, unrelated to quantum computers, are also discussed.

The main requirements for an encapsulated donor atom to serve as a solid-state qubit in any architecture for a quantum computer are the following. First, the donor atom shall have a  $\frac{1}{2}$  nuclear spin and an s like donor electron with reasonable nuclear spin-electron coupling. Second, the donor electronic state shall not be too tightly bound to the location of the atom. Third, the encapsulated donor atoms of larger sizes shall be configurationally very stable against diffusion during and after the fabrication steps. Additionally, fourth, we require that any proposed scheme shall also have reasonably demonstrated experimental steps contributing towards possible fabrication pathways. Based on these four requirements, in this work, we propose and examine below two models of encapsulated nuclear spin  $\frac{1}{2}$  atoms to serve as individual qubits in a solid-state quantum computer. [8-10] Coupling between neighboring qubits, either directly through diamond lattice or through any high K dielectric host lattice, is currently under investigation and will be described elsewhere.

The first model involves encapsulating a nuclear spin  $\frac{1}{2}$   $^1\text{H}$  atom in a fullerene, and the second model envisions encapsulating a  $^{31}\text{P}$  atom in a few nanometer sized diamond nanocrystallite to serve as single qubits. Arrays of such larger sized qubits could be envisioned for future quantum computer applications.

**Model 1:  $^1\text{H}$  atom encapsulated in a Fullerene** — To realize a nuclear spin based solid-state qubit,  $\frac{1}{2}$  nuclear spin and strong nuclear spin-electron coupling are necessary conditions. One of the most promising candidates is atomic  $^1\text{H}$  because it has  $\frac{1}{2}$  nuclear spin (except in deuterium) and there is one valence electron in the s orbital that is tightly bound to the nuclear position with strong nuclear spin-electron coupling. However, the main challenge is that the atomic  $^1\text{H}$  is very reactive and easily forms a covalent bond to become a molecular or chemisorbed species. The only available valance electron will be used up in the reaction and not available for hyperfine contact coupling to the nuclear spin. Additionally, even if the  $^1\text{H}$  atom can be kept in an atomic state, maintaining its position in a bulk lattice could be very difficult because  $^1\text{H}$  is lightweight atom and is highly mobile even at very low temperatures. Therefore, a  $^1\text{H}$  atom may not be suitable for a qubit application unless; (a) it can be kept in atomic state with in a solid-state system, and (b) its mobility is also reduced significantly. Encapsulating a  $^1\text{H}$  atom within a fullerene could be a solution to satisfy the above conditions.

The internal chemical reactivity of fullerenes was first examined in order to verify if a  $^1\text{H}$  atom can stay in an atomic state within a fullerene. The internal hydrogenation of a variety of fullerenes was examined with *ab-initio* density functional theory [DFT] pseudo-potential methods. [11] For this study, we have examined two fullerenes,  $\text{C}_{36}$  [12] and  $\text{C}_{60}$  [13], and the main findings are as follows. There are several isomers for  $\text{C}_{36}$  and we have chosen to use  $\text{C}_{36} D_{6h}$ , which is known to be the most stable isomer [12, 14]. The intrinsic structures of  $\text{C}_{36}$  and  $\text{C}_{60}$  were optimized using DFT pseudo-potential method, [11] and are shown in Figs. 1 (a) and (b), respectively.  $\text{C}_{36}$  has three different types of C atom sites and  $\text{C}_{60}$  has one type of C atom site as indicated in the figure. All possible reactions of a  $^1\text{H}$  atom with the internal binding sites of the fullerene-wall C atoms were examined, and the results are summarized in Table 1.

When a  $^1\text{H}$  atom is placed at the center of  $\text{C}_{36}$  or  $\text{C}_{60}$  fullerene, it has about  $-0.45$  eV binding energy and the valence electron remains in atomic state localized at the center. Fig. 1 (c) shows that  $^1\text{H}$  atom stays at the center of  $\text{C}_{36}$  and that the valence electron of the  $^1\text{H}$  atom is well localized around the  $^1\text{H}$  atom. Even though there are no significant bonds around the  $^1\text{H}$  atom, the sum of small interactions (about  $-0.013$  eV per C atom) between the  $^1\text{H}$  atom and the surrounding 36 C atoms contribute towards negative binding energy of  $-0.46$  eV. However, the  $^1\text{H}$  atom at the center is a meta-stable minimum energy configuration. In the global minimum energy configuration, the  $^1\text{H}$  atom forms a covalent bond with the fullerene-wall carbon atom as shown in Fig. 1(d). The global minimum energy configuration at the fullerene-wall C atom is energetically more stable than the  $^1\text{H}$  atom at the center by about 1 eV in both fullerenes. Similar results were found for other fullerenes studied.

In general, the internal surfaces of fullerenes are relatively inert, and there are several successful examples of capturing an atom inside a fullerene without forming covalent bond with a fullerene-wall C atom. [15,16] However,  $^1\text{H}$  atoms are highly reactive so that the wall C atoms can form covalent bonds with encapsulated  $^1\text{H}$  atom. Thus the encapsulated  $^1\text{H}$  atom, if prepared, is most likely to react with the wall C atoms and will not have strong enough hyperfine contact coupling for qubit application. This situation can be reversed if one can reduce the internal chemical reactivity of the fullerene-wall C atoms. Since the internal

and external reactivity of the fullerene-wall C atoms is due to  $\pi$  electron density, which has mixed hybridization (between  $sp^2$  and  $sp^3$ ) of the wall C atoms [17], the internal reactivity could be reduced by removing the  $\pi$  electron density of the wall C atoms. In general this can be achieved by the hydrogenation of the exterior of the wall C atoms of the fullerene. The external hydrogenation would remove the most reactive  $\pi$  electron states from the interior so that a  $^1\text{H}$  atom could be stable at the center.

As an example, the encapsulation of a  $^1\text{H}$  atom in a dodecahedrane  $\text{C}_{20}\text{H}_{20}$ , which is shown in Fig. 2 (a), was investigated. The changes in the binding energy of a  $^1\text{H}$  atom on internal surface of  $\text{C}_{20}\text{H}_{20}$  were calculated. The  $\text{C}_{20}\text{H}_{20}$  hydrogenated-fullerene has 3 high symmetry binding sites on the internal surface of the fullerene. The three sites are on top of the C atoms, on the center of bonds between the C atoms, and on the center of C atom pentagon rings. Binding energies along all the three sites were computed as a function of the distance from the center and the results are shown in Fig. 2 (b). Since all the C atoms are now fully saturated with four covalent bonds (of  $sp^3$  type), there is no binding between the  $^1\text{H}$  atom and internal surface of the fullerene. As a result Fig. 2 (b) shows that the  $^1\text{H}$  atom at the center site is the global minimum energy configuration and that there is no meta-stable minimum energy configuration. The energetics of a possible diffusion path of  $^1\text{H}$  atom from the center of  $\text{C}_{20}\text{H}_{20}$  to the center of a fullerene-wall pentagon shows that the barrier to escape from the fullerene is about 1 eV though the pentagons. This result is consistent with some other recent experimental [18] and theoretical [19] studies.

The spatial distribution of the valance electron of the encapsulated  $^1\text{H}$  atom within  $\text{C}_{20}\text{H}_{20}$  was also studied. This will be needed to estimate the coupling between neighboring qubits through valance electron overlaps of the neighboring qubits. If the valance electron wave function is totally trapped or shielded within the encapsulating fullerene ( $\text{C}_{20}\text{H}_{20}$ ), the above model will not be useful for more than single qubit system. Figure 2 (c) shows that the valance electron density of the  $^1\text{H}$  atom encapsulated within  $\text{C}_{20}\text{H}_{20}$ , which is mostly concentrated at the center. Drawn at a different scale in Fig. 2 (d) the valance electron density is shown to be leaking outside of the encapsulating fullerene. This indicates that the  $sp^3$  bonded fullerene shell increase the range of electron distribution through a dielectric screening similar to a diamond lattice ( $\epsilon = 6$ ).

The high valance electron density region at the center is removed and shown as a blank due to the scale of the electronic density plotted in Fig. 2(d). When the  $^1\text{H}$  atoms on the outer surface of  $\text{C}_{20}\text{H}_{20}$  are replaced with deuterium  $^2\text{D}$  atoms, the valance electron density plots remain same as shown in Fig. 2 (c) and (d). Additionally, the advantage is that the deuterium  $^2\text{D}$  atoms do not have nuclear spin and cannot interfere in any nuclear spin related measurements on the model 1 of the qubit ( $^1\text{H} @ \text{C}_{20}\text{D}_{20}$ ) proposed in this work.

***Model 2:  $^{31}\text{P}$  atom encapsulated in a Diamond Nanocrystallite :***

A  $^{31}\text{P}$  atom has  $\frac{1}{2}$  nuclear spin and is the only natural isotope. When it is used as a dopant in any diamond lattice structured materials (e.g. Group IV elements in the periodic table), its four valence electrons participate in making tetrahedral covalent bonds. The fifth electron exists in a weakly bound s-like orbital within the lattice. Using this property, a conceptual design of solid-state quantum computer based on arrays of  $^{31}\text{P}$  atoms in bulk Si, has been proposed by Kane. [7] As discussed above, the major obstacle of this proposal is the experimental difficulty in fabricating of arrays of donor atom dopants,  $^{31}\text{P}$ , beneath Si surface layers and the stability of dopant atoms. A possible solution to overcome these difficulties would be to encapsulate the  $^{31}\text{P}$  atom in a diamond nanocrystallite (2-10 nm sized) in a similar way as suggested  $^{31}\text{P}$  substitutional doping in bulk silicon, and use the doped nanocrystallite as a single qubit. The main requirements for a  $^{31}\text{P}$  doped diamond nanocrystallite to work as a single qubit are: (a) a  $^{31}\text{P}$  doped at a substitutional site in a diamond nanocrystallite shall be a stable structure with no or minimal possibility of diffusion to the nanocrystallite surface, (b) weakly bound donor electron in the lattice shall be strongly coupled to nuclear spin through hyperfine contact interaction, (c) the donor electron wave function in the lattice shall have sufficient spread to allow for a coupling between neighboring qubits, and (d) fabrication pathways for  $^{31}\text{P}$  doping in a diamond nanocrystallite shall be experimentally feasible.

It turns out that the proposed model of  $^{31}\text{P}$  doped in a diamond nanocrystallite can be fabricated through experimentally feasible steps as we have suggested recently. [8-10] The steps are: (a) encapsulate a  $^{31}\text{P}$  atom at the center of a fullerene to make an endofullerene,  $^{31}\text{P}@ \text{C}_{60}$ , (b) use the thus generated endo-fullerene to grow bucky-onion (concentric graphitic spherical shells) layers on the endo-fullerene, (c) use an e-beam

irradiation on the outer most bucky onion layers, followed by annealing of the system, to convert the core layers into a diamond nanocrystallite with a  $^{31}\text{P}$  atom trapped at the center, (d) chemically clean the remaining bucky onion layers to finally get a diamond nanocrystallite doped with a single  $^{31}\text{P}$  donor atom at the center. The energetic, structural and electronic behaviors of these processes involved in the above steps are examined with DFT pseudo-potential methods. [11]

The first step of encapsulating a  $^{31}\text{P}$  atom in a variety of fullerenes has been investigated for stability and the positioning of the  $^{31}\text{P}$  atom inside fullerenes. Since  $\text{C}_{60}$  is a seed material for bucky onion growth, we focus our discussion on the encapsulation of  $^{31}\text{P}$  atom in a  $\text{C}_{60}$  fullerene. A  $^{31}\text{P}$  atom was inserted within a fullerene and structural stability, binding sites and electronic properties were investigated. Two energetically stable configurations are identified such that the  $^{31}\text{P}$  atom either stays at the center of  $\text{C}_{60}$  or on top of a C-C bond that connect two pentagons on the wall of  $\text{C}_{60}$ . The binding energies are  $-0.99$  eV and  $-0.81$  eV for center site and on bond top site, respectively. Therefore  $^{31}\text{P}$  atom will stay at the center of the fullerene. Recently there have been experiments to put  $^{31}\text{P}$  atom in  $\text{C}_{60}$  using ion implantation method. [16] Experimentally, it is found that  $^{31}\text{P}$  is most likely to be at the center of  $\text{C}_{60}$ . This is in agreement with our results based on DFT pseudo-potential method. The electron density of the donor electron in  $^{31}\text{P}$  in  $\text{C}_{60}$ , shown in Fig. 3 (a), exhibits a well-isolated  $^{31}\text{P}$  atom at the center of  $\text{C}_{60}$  fullerene, hence the thus impregnated  $^{31}\text{P}$  @  $\text{C}_{60}$  fullerene is suitable as a seed material for growing bucky onion layers.

The step of converting core layers of a bucky onion into diamond nanocrystallite at pressures above 20 GPa has already been demonstrated in experiments. [20, 21] This is done by inflicting e-beam irradiation induced defects and etching in outer most shells of the bucky onions. During the annealing process, defected outer shells with reduced number of C atoms form smaller radii, and consequently exert an inward hydrostatic compression, as much as 50 ~ 150 GPa, on the inner core shell layers. At such high pressures graphitic to diamond structural transition occurs creating a diamond nanocrystallite of 2-50 nm diameter. [21] Further more, experiments have found single crystal diamond formation in smaller sized (2-10 nm) crystallite, and polycrystalline diamond formation in larger sized crystallite. Through DFT pseudo-potential

calculations we have examined the structural and electronic properties of the  $^{31}\text{P}$  atom substituted in a regular and compressed diamond nanocrystallite.

To gauge the most likely configuration of  $^{31}\text{P}$  atom during the nanocrystallite formation process, we have examined the formation energy and structural configuration of  $^{31}\text{P}$  doped in a diamond nanocrystallite for three most possible configurations with  $^{31}\text{P}$  at a substitutional site, a  $^{31}\text{P}$  at hexagonal or tetrahedral interstitial sites. The hydrostatic pressure on the diamond nanocrystallite was varied from 0 to 50 GPa to simulate appropriate scaling down of the diamond lattice parameters during high pressure processing. The main results are summarized in Table 2. As the pressure increases, the formation energies of all the  $^{31}\text{P}$  doped configurations increase. This is natural because the  $^{31}\text{P}$  atom is bigger than the lattice C atom, and there is increasingly less space for the  $^{31}\text{P}$  in the lattice as pressure increases. Results in Table 2 show that the  $^{31}\text{P}$  at the substitutional site is the most stable configuration even in the highly compressed diamond lattices. The energy required to hop from a substitutional site to a hexagonal or tetrahedral interstitial sites is also much higher than the corresponding energy for a  $^{31}\text{P}$  atom in a silicon lattice. This means that even though a  $^{31}\text{P}$  at the substitutional site of a diamond lattice has a small positive formation energy, (0.88 eV) relative to the phase separated diamond and bulk  $^{31}\text{P}$ , the  $^{31}\text{P}$  atom, once substituted via our proposed trapping mechanism, will stay because of very large energy barriers to diffuse out of the nanocrystallite.

The thermal stability of the  $^{31}\text{P}$  atom at a substitution site configuration, against diffusion, was tested by computing the vacancy and interstitial formation energies. Both of these intrinsic defects play key role in the diffusion of atomic species in bulk semiconductor materials. [22] The results are summarized in Table 2. The vacancy formation energy is fairly high (over 6 eV) and is not favorable to be produced naturally during any process. The vacancy formation energy changes only very slightly as the pressure goes up. The self-interstitial formation energy would be even higher than vacancy formation energy due to small atomic space in diamond lattice. The Table 2 also shows the formation energies of  $^{31}\text{P}$  atom at interstitial sites, which can be formed by C self-interstitial defect and provide other important mechanisms of diffusion. The  $^{31}\text{P}$  at a substitutional site of diamond is more favorable than any other interstitial sites by over 15 eV, which

provides a large amount of energy barrier against diffusion through self-interstitial mediated kick-out mechanism. For a comparison, the interstitial formation energy of a  $^{31}\text{P}$  atom relative to a substitutional site is only around 3 eV in bulk silicon. In Si lattice both vacancy and self-interstitial defects have relatively low formation energy of 3–4 eV, and both vacancy and interstitial mediated diffusion in Si are known to occur during the processing steps. This analysis shows that  $^{31}\text{P}$  in diamond nanocrystallite based arrays, if fabricated, will be much more stable against any diffusion mediated disruption mechanism than  $^{31}\text{P}$  atoms in silicon lattice.

Lastly, the donor electron density of the  $^{31}\text{P}$  atom at the substitutional site within the diamond lattice is shown in Fig. 3b. For brevity, we show the planar donor electron density profile in the (111) plane of the underlying diamond lattice structure. The electron density profile in the (111) plane is nearly symmetric and does not decay exponentially as expected for an isolated donor electron atom. Moreover, we found that the decay profile of the donor electron density within a diamond lattice structure is anisotropic and channeled favorably along certain lattice directions and not so favorably along other lattice directions. A detailed analysis of this property to facilitate inter-qubit coupling is currently underway and will be published elsewhere.

For a single qubit model, in this work, the only possible difference comes from changing the host material from bulk Si to diamond. The dielectric constant of diamond ( $\epsilon = 5.5$ ) is half of that of bulk Si ( $\epsilon = 11.7$ ) and effective mass of electron in diamond is of the same order as that of in bulk Si ( $m_{\text{eff}}/m = 0.2$ ). Therefore we estimate that the hyperfine coupling ( $A \propto \epsilon^{-3}$ ) needed to control a nuclear spin on a single qubit, through an electric field applied by an external gate, in our model is about 8 times stronger than the coupling in Kane's silicon-based model. This means that one could, in principle, use a weaker electric field, for the same level of control, than the field required in Kane's model and that the inter-qubit exchange frequency ( $\nu \propto A^2$ ) will increase by two orders of magnitude. On the other hand, donor electron density overlap between neighboring qubits, in bulk diamond reduces by a factor of 2 as compared to that in bulk silicon ( $a_B \propto \epsilon$ ). The neighboring qubit interactions in our case thus would be weaker by the same factor as

compared to the interactions proposed in Kane's model. This shows that the above-proposed model for a single qubit is well within the range of operating conditions elucidated by Kane. The detailed analyses involving more than single qubit structures is currently underway and will be published elsewhere.

### **Comments:**

In summary, two models of using nuclear spin states of encapsulated atoms in fullerenes and diamond nanocrystallite are proposed and examined through ab-initio DFT pseudo-potential method. The first model shows that a nuclear spin  $\frac{1}{2}$   $^1\text{H}$  atom remains stable at the center of a  $\text{C}_{20}\text{D}_{20}$  (deuterated) fullerene with a barrier of about 1 eV for the encapsulated  $^1\text{H}$  atom to diffuse out of the qubit unit. In the second model, the formation energy of a  $^{31}\text{P}$  atom at the substitutional site in a diamond nanocrystallite is found to be significantly less than the formation energies of vacancy (by 6 eV) and  $^{31}\text{P}$  at interstitial (by 15 eV) sites. This proves that a  $^{31}\text{P}$  atom, if substituted with in a diamond nanocrystallite, is much more stable than the similar substitution in bulk Si. The strength of hyperfine contact coupling for controlling a qubit, via an external electric field, has increased in our model while the electron-electron coupling depending on the donor electron overlaps requires a shorter inter qubit distance. The nature and spatial extension of the electronic wave functions in the two models are found to be satisfactory for single qubit application. Furthermore, the detailed analysis of the donor electron density channeling through a diamond lattice structure, important for two or more than two qubit systems, is currently underway and will be published elsewhere. The experimental fabrication steps needed to fabricate single qubits are elucidated, and we have confirmed that these experiments have been already performed separately for different nanotechnology applications without any connection to quantum computing.

### **Acknowledgements:**

The research performed is supported by NASA Ames Director's Discretionary Fund (DDF) Award to DS (NASA Ames) and KC(Stanford). Authors thank TR Govindan, Vadim Smylenski and Dogan Timucin (all at NASA Ames) for significant discussion, and DS is supported by NASA contract 704-40-32 to CSC. The DFT simulations are performed under the NPACI allocation SUA239 "Nanoscale Materials Simulations."

Table 1 Hydrogenation of  $C_{60}$  and  $C_{36}$

$C_{36}$				$C_{60}$	
Carbon A	Carbon B	Carbon C	Center	Carbon	Center
-1.28	-1.54	-1.40	-0.46	-1.23	-0.43

Table 2 Formation energies

	0 GPa	20 GPa	50 GPa	Si
Substitutional site	0.88	1.99	3.85	-5.75
Hexagonal site	15.95	18.26	21.99	-2.71
Tetrahedral site	19.13	21.53	25.35	-1.90
Vacancy	6.78	6.65	6.65	

## References:

1. See for example a recent review by Steane A, "Quantum Computing," *Rep. Prog. Phys.* **B61**, 117–173 (1998).
2. Ekert A and Jozsa R, "Quantum Computation and Shor's Factoring Algorithm," *Rev. Mod. Phys.* **B68**, 733–753 (1996).
3. Grover LK, "Quantum mechanics helps in searching for a needle in a haystack," *Phys. Rev. Lett.* **79**, 325–328 (1997).
4. Preskill J, "Reliable Quantum Computers," *Proc. R. Soc. London A* **454**, 385–410 (1998).
5. Gershenfeld NA and Chuang IL, "Bulk Spin Resonance Quantum Computations," *Science* **275**, 350–356 (1997).
6. Chung IL, Vandersypen LMK, Zhou XL, Leung DW and Lloyd S, "Experimental realization of a quantum algorithm," *Nature* **393**, 143–146 (1998)
7. Kane BE, "A silicon-based nuclear spin quantum computer", *Nature* **393**, 133–137 (1998)
8. D. Srivastava, K. Cho and T. R. Govindan, DDF Proposal, "Simulation based Prototyping of Solid-State Quantum Computers: A Pathway for Revolutionary Computing in the 21<sup>st</sup> Century," (May 99 – Dec 2000)
9. S. Park, D. Srivastava and K. Cho, "Carbon based Nanotechnology for Solid-State Quantum Bits," manuscript submitted to *Nature* (2001)
10. S. Park, D. Srivastava and K. Cho, "Local Reactivity of Fullerenes and Applications to a Nanodevice Design," manuscript submitted to the Special Issue of *Nanotechnology* (2000)
11. See for a review of DFT simulation method, Payne MC, Teter MP, Allan DC, Arias TA and Joannopoulos JD, "Iterative minimization techniques for *ab initio* total-energy calculations: molecular-dynamics and conjugate gradients" *Rev. Mod. Phys.* **64** 1045–1097 (1992)
12. Piskoti C, Yarger J and Zettl A, "C<sub>36</sub>, a new carbon solid," *Nature* **393**, 771–774 (1998)
13. Kroto HW, HEATH JR, OBRIEN SC, CURL RF and SMALLEY RE, "C<sub>60</sub>: Buckminsterfullerene," *Nature* **318**, 162–163 (1985)
14. Grossman JC, Côté M, Louie ST, and Cohen ML, "Electronic and structural properties of molecular C<sub>36</sub>," *Chemical Physics Letters* **284**, 344–349 (1998)

15. Murphy TA, Pawlik T, Weidinger A, Hohne M, Alcala R and Spaeth JM, "Observation of atomlike nitrogen in nitrogen-implanted solid C<sub>60</sub>," *Physical Review Letters* **77**, 1075–1078 (1996)
16. Knapp C, Weiden N, Kass K, Dinse KP, Pietzak B, Waiblinger M and Weidinger A, "Electron paramagnetic resonance study of atomic phosphorus encapsulated in C<sub>60</sub> fullerene," *Molecular Physics* **95**, 999-1004 (1998)
17. Hirsch A, "Principles of fullerene reactivity," *Topics in Current Chemistry* **198**, 1–65 (1998)
18. Cross RJ, Saunders M and Prinzbach H, "Putting helium inside dodecahedrane," *Organic Lett.* **1**, 1479–1481 (1999)
19. Dixon DA, Deerfield D, Graham GD, "The electronic-structure of dodecahedrane and the nature of the central cavity," *Chemical Physics Letters* **78**, 161–164 (1981)
20. Regueiro MN, Monceau P and Hodeau JL, "Crushing C<sub>60</sub> to diamond at room-temperature," *Nature* **355**, 237–239 (1992)
21. Banhart F and Ajayan PM, "Carbon onions as nanoscopic pressure cells for diamond formation," *Nature* **382**, 433–435 (1996)
22. Fahey, PM, Griffin, PB and Plummer, JD, "Point-defects and dopant diffusion in silicon" *Reviews of Modern Physics* **61**, 289–384 (1989)

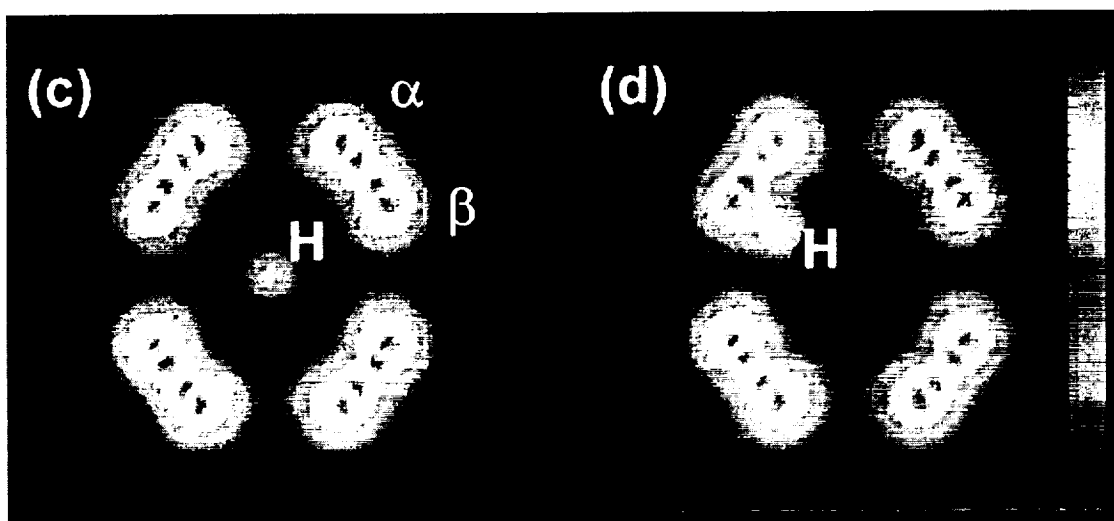
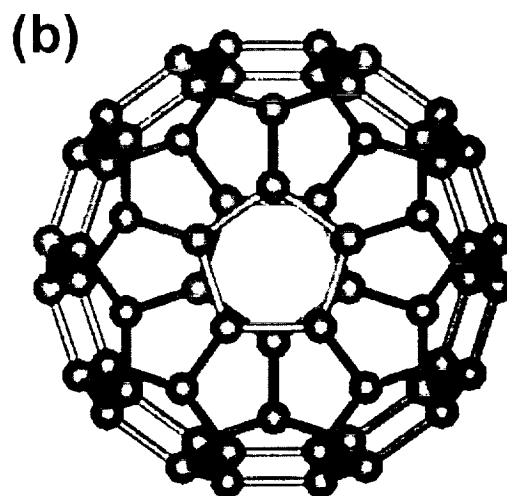
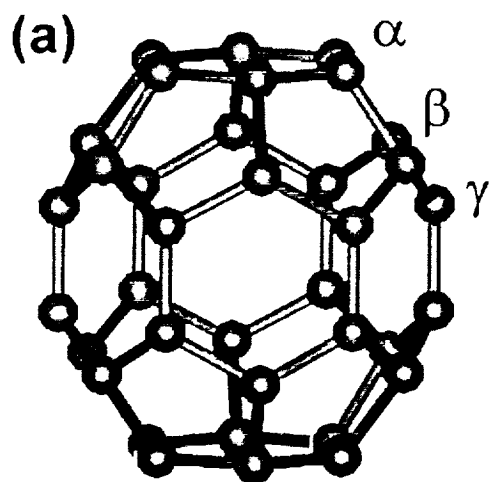


Figure 1

(a) Atomic structure of  $C_{36}$ , different types of C atoms are name by  $\alpha$ ,  $\beta$  and  $\gamma$ , (b) atomic structure of  $C_{60}$ , (c) charge density of H at the center of  $C_{36}$ , which shows carbon  $\alpha$  and  $\beta$ , (d) charge density of H on carbon  $\beta$  of  $C_{36}$

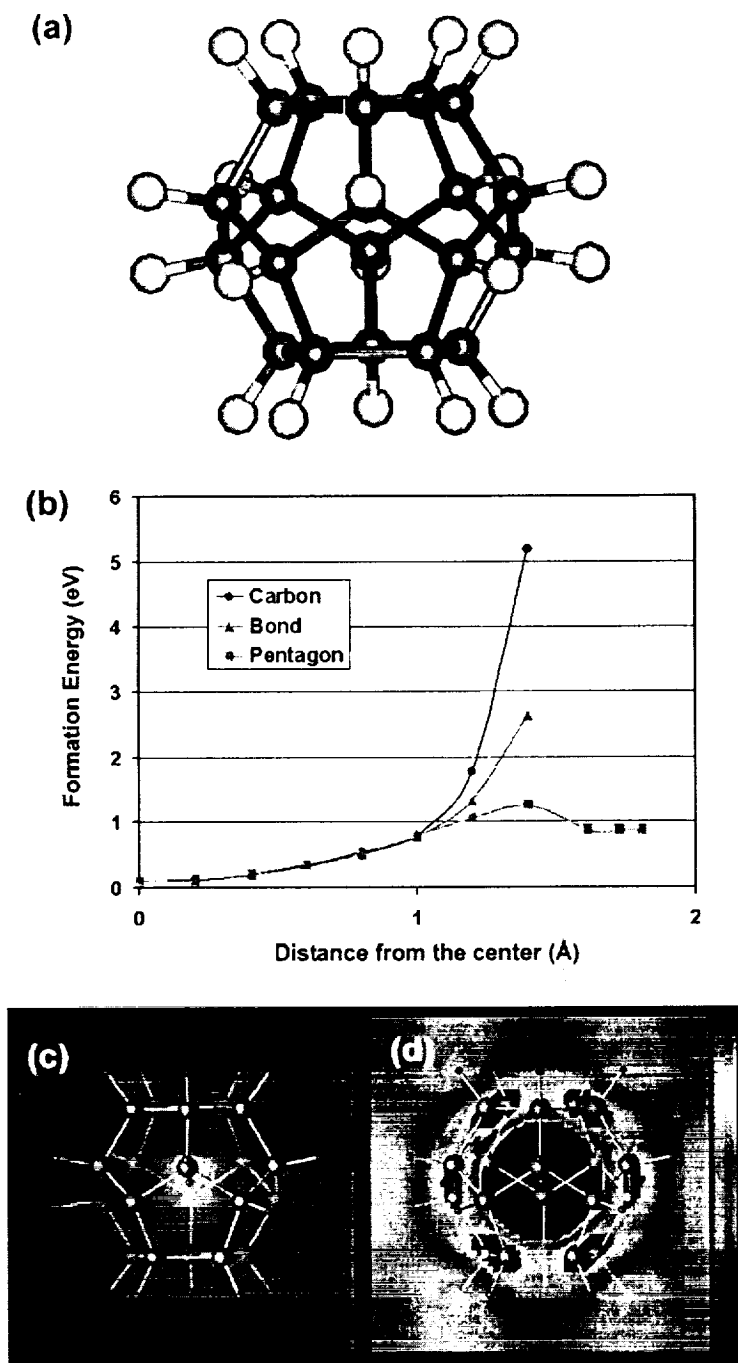


Figure 2  
 (a) Atomic structure of  $C_{20}H_{20}$ , (b) atomic structure of  $C_{20}H_{20}$ , (c) valence electron density of atomic H at  $C_{20}H_{20}$ , (d) valence electron density of atomic H at  $C_{20}H_{20}$  at 300 times magnified scale as compared to (c), fullerene structure induced leaking of electron density out of the encapsulating structure is shown.

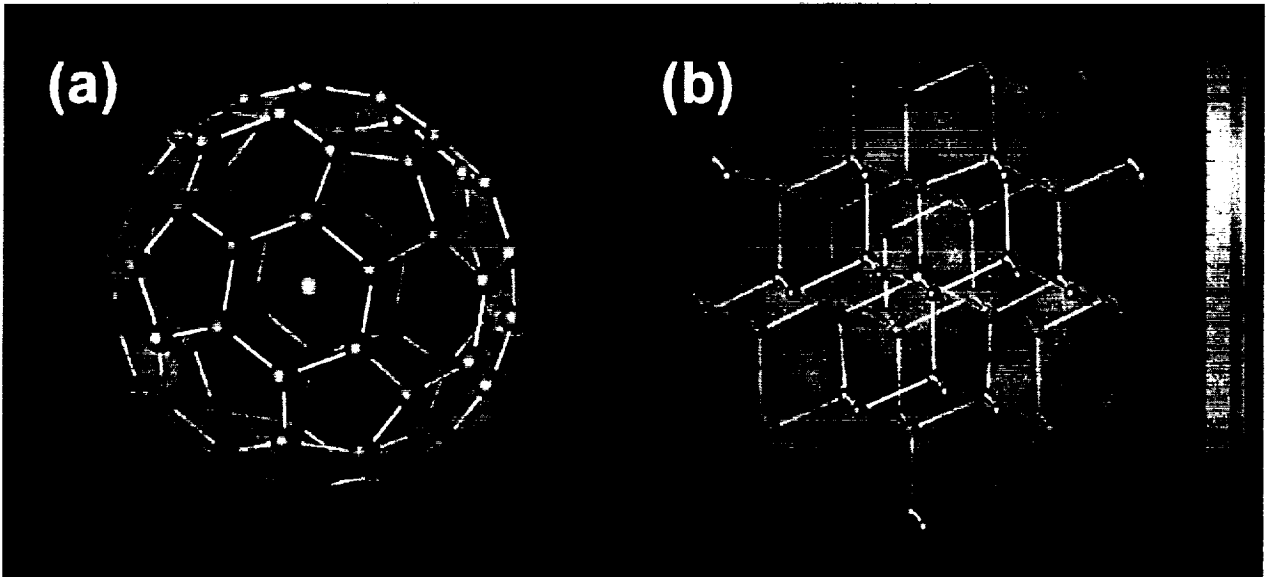


Figure 3  
(a) Electron density of <sup>31</sup>P stable at the center of C<sub>60</sub> fullerene, and (b) donor electron density of <sup>31</sup>P in a diamond nanocrystallite shown in a (111) plane.